AIP | Journal of Applied Physics

Structural tunability and switchable exciton emission in inorganic-organic hybrids with mixed halides

Shahab Ahmad, Jeremy J. Baumberg, and G. Vijaya Prakash

Citation: Journal of Applied Physics **114**, 233511 (2013); doi: 10.1063/1.4851715
View online: http://dx.doi.org/10.1063/1.4851715
View Table of Contents: http://scitation.aip.org/content/aip/journal/jap/114/23?ver=pdfcov
Published by the AIP Publishing

Structural tunability and switchable exciton emission in inorganic-organic hybrids with mixed halides

Shahab Ahmad,[1] Jeremy J. Baumberg,[2] and G. Vijaya Prakash[1,a)]
[1]*Nanophotonics Lab, Department of Physics, Indian Institute of Technology Delhi, New Delhi 110016, India*
[2]*Nanophotonics Centre, Cavendish Laboratory, University of Cambridge, Cambridge CB3 0HE, United Kingdom*

(Received 12 October 2013; accepted 4 December 2013; published online 20 December 2013)

Room-temperature tunable excitonic photoluminescence is demonstrated in alloy-tuned layered Inorganic-Organic (IO) hybrids, $(C_{12}H_{25}NH_3)_2PbI_{4(1-y)}Br_{4y}$ (y = 0 to 1). These perovskite IO hybrids adopt structures with alternating stacks of low-dimensional inorganic and organic layers, considered to be naturally self-assembled multiple quantum wells. These systems resemble stacked monolayer 2D semiconductors since no interlayer coupling exists. Thin films of IO hybrids exhibit sharp and strong photoluminescence (PL) at room-temperature due to stable excitons formed within the low-dimensional inorganic layers. Systematic variation in the observed exciton PL from 510 nm to 350 nm as the alloy composition is changed, is attributed to the structural readjustment of crystal packing upon increase of the Br content in the Pb-I inorganic network. The energy separation between exciton absorption and PL is attributed to the modified exciton density of states and diffusion of excitons from relatively higher energy states corresponding to bromine rich sites towards the lower energy iodine sites. Apart from compositional fluctuations, these excitons show remarkable reversible flips at temperature-induced phase transitions. All the results are successfully correlated with thermal and structural studies. Such structural engineering flexibility in these hybrids allows selective tuning of desirable exciton properties within suitable operating temperature ranges. Such wide-range PL tunability and reversible exciton switching in these novel IO hybrids paves the way to potential applications in new generation of optoelectronic devices.
 [http://dx.doi.org/10.1063/1.4851715]

I. INTRODUCTION

Low-dimensional hybrid materials with quantum confinement have attracted considerable attention due to the possibility of creating exploitable low-cost optoelectronic devices. One of the most interesting category of hybrid materials is a *perovskite* type inorganic-organic (IO) hybrid. These perovskite type IO hybrids are self-organized layered materials which adopt a generic structural formula of AMX_3 (A is organic moiety, M is divalent metal: Pb^{2+}, Sn^{2+}, Ge^{2+}, and X is halide: I^-, Br^-, Cl^-).[1–3] Their unique crystal structures offer flexibility in the choice of several types of organic spacers, so that the crystallographic conformations can be appropriately tailored.

Lead (II) halide based inorganic-organic layered perovskite compounds, with a general formula $(R\text{-}NH_3)_2PbX_4$ (R: $C_nH_{2n+1}^-$, $C_6H_5C_nH_{2n}^-$, X: Cl, Br and I),[4,5] are environmentally benign and self-assembled systems.[6,7] The general structure of these IO hybrids consists of layers of corner-sharing PbX_6 octahedra alternating with layers of $R\text{-}NH_3$ cations with NH_3 ammonium groups linked to the inorganic layers by three charge assisted N–H—X hydrogen bonds.[6–9] Such IO hybrids form "natural" multiple quantum-well structures (MQW), where "wells" of 2D inorganic semiconducting layers are clad by "barriers" of the organic layers and show both quantum and dielectric confinement effects.[7] As a consequence, stable room-temperature excitons are formed within the inorganic layer having enhanced binding energies of up to few hundreds of meV, about four times larger than 3-D counterpart and the oscillator strength becomes larger than the bulk exciton.[7,10,11] These strong room-temperature excitonic features have thermal stability even up to 200 °C and are most favorable for many optoelectronic applications, such as light emitting diodes (IO-LED), thin film field-effect transistors (IO-TFTs), and nonlinear optical switches based on strong exciton-photon coupling in microcavity photonic architectures.[12–14] These structures resemble 2D semiconductor monolayers, where the sheets are uncoupled and can be easily solution-casted over large areas.[15,16]

Structural engineering and electronic band structure of these IO hybrids can be tailored systematically either by changing the divalent metal, halogen species or organic moiety.[2,12] For example, in ML_4^{2-} type IO hybrid systems replacement of $M = Pb^{2+}$ to Sn^{2+}, shifts the exciton emission substantially from 520 nm to 630 nm,[17,18] (however, at the cost of great sensitivity to environmental oxygen). Similarly in PbX_4^{2-} systems, the replacement of halide (X^-) species from I^- to Br^- to Cl^-, tunes the excitons from 520 nm to 280 nm.[8,19–22] Replacement with various organic moiety spacers in PbI_4^{2-} system shows the effects of conformation directly on the PbI network with about 10–20 nm wavelength variation in their exciton features.[8,23,24] Recently, it was demonstrated in amino-based long-alkyl chain IO hybrids, $(C_nH_{2n+1}NH_3)_2\ PbI_4$ (n = 12,16,18), that

a)Author to whom all correspondence should be addressed. Electronic mail: prakash@physics.iitd.ac.in.

the conformation of organic moiety alignment from *trans* to *gauche* (and vice-versa) into the inorganic (Pb-I) network further induces flexibility in creating reversible structural phase transitions at easily accessible device temperatures, and as a result reversible exciton emission switching between two types of excitons is observed.[25,26] In general, optical, electronic and structural features of these hybrids are critically dependent upon network formation of M-X bonds in the perovskite layers, and the conformation of the organic moiety that links the two layers through hydrogen bonding at the ammonium head-group. The engineering flexibility of the emission properties arises from appropriate design of these bridging organics and adjustment of the M-X environment. Therefore, exciton behavior in IO hybrids containing mixed-alloy inorganic networks and also their reversible structural phase transitions is complex to understand but offers a unique system of structurally responsive and tunable excitons.

Here, the systematic study of long-alkyl-chain containing mixed lead (II) halide IO hybrid $(C_{12}H_{25}NH_3)_2PbI_{4(1-y)}Br_{4y}$ systems with systematic variation from I^- to Br^- is presented. We describe the large-area rapid and cost-effective synthesis of $(C_{12}H_{25}NH_3)_2PbI_{4(1-y)}Br_{4y}$ mixed IO hybrids and the systematic correlation between structural and thermal properties to the observed strong room-temperature exciton features and optical properties. These results exemplify the wide range of exciton tunability that arises due to structural engineering of metal halides. Such critical understanding of opto-thermo-structural properties in these novel IO hybrids is relevant to stability and device potential for low-cost and next-generation optoelectronic applications.

II. EXPERIMENTAL METHODS

Thin films of IO hybrids $(C_{12}H_{25}NH_3)_2PbI_{4(1-y)}Br_{4y}$ ($y = 0$ to 1) were synthesized using conventional solution-processing methods.[8,20,23] First, $(C_{12}H_{25}NH_3)X$ (X = I or Br, hereafter C12I, C12B, respectively) was synthesized from the mixture of aqueous solutions of HX (HI or HBr) and dodecylamine ($C_{12}H_{25}NH_2$). The precipitate from the reactant solution was separated and then washed with diethyl ether. For hybrids at $y = 0.0$ and 1.0, stoichiometric amounts of $(C_{12}H_{25}NH_3)X$ (X = I or Br) and corresponding lead halide (PbI_2 or $PbBr_2$) were dissolved in N,N-dimethylformamide (DMF) (hereafter, the resultant compounds are termed C12PI and C12PB, respectively). For intermediate compounds of $y = 0.37$ and 0.62 suitable stoichiometric amounts of C12I, C12B, PbI_2, and $PbBr_2$ were used as the starting materials. The supernatant solutions are spin-coated or drop-cast on to pre-heated (50 °C) glass substrates to obtain required thin films. For thermal measurements, the required powders are extracted from the supernatant solutions. Thin film absorption measurements were carried out using a white light source coupled to a fiber optic spectrometer. Photoluminescence (PL) measurements were carried out using a 337 nm N_2 laser (~10 mW) as excitation source and the emission is coupled into a monochromator coupled with a PMT or fiber-optic spectrometers, using appropriate filters. The PL images and spectral spatial maps are obtained from a modified microscope equipped with XY-piezo stage, 404 nm diode laser (<50 mW) and fiber-optic spectrometer using a long-pass ($\lambda > 410$ nm) filter. For temperature-dependent PL, a sample holder equipped with temperature controller has been used. Differential Scanning Calorimetry (DSC) studies on powder samples were performed within the temperature range from 0 °C to 120 °C at a rate of 5 °C/min in both heating and cooling runs. Glancing angle thin film X-Ray Diffraction studies were carried out in the 2θ range from 3° to 40° with Cu Kα radiation ($\lambda = 1.5406$ Å).

III. RESULTS

The phase purity, crystallinity and structural rearrangements of the prepared $(C_{12}H_{25}NH_3)_2PbI_{4(1-y)}Br_{4y}$ ($y = 0$–1) [hereafter C12PbI$_{4(1-y)}$Br$_{4y}$] thin films were characterized by glancing angle X-ray diffraction (GAXRD) techniques at room-temperature. Fig. 1(b) shows the obtained X-ray diffraction patterns of thin films, with strong diffraction peaks corresponding to higher order (0 0 2l) reflections showing that the C12PbI$_{4(1-y)}$Br$_{4y}$ thin films are highly oriented, with the c-axis perpendicular to the substrate surface.[21] Further, a systematic shift in the (0 0 2l) peak towards lower diffraction angles with increasing bromine content has also been observed (Fig. 1(b), inset). The detailed crystal structure of C12PI ($y = 0.0$) single crystals has been reported by us recently and is thus only briefly discussed here.[8] The structural packing of C12PI shows the formation of a layered structure stacked along the c-axis with alternate stacking of PbI_4^{2-} and alkyl ammonium based organic moieties $(C_{12}H_{25}NH_3)I$, while both networks are infinitely extended in the ab-plane. Structural studies of R-PbX$_4$ (X = I, Br, Cl) type layered hybrids are of special interest and have been well studied in the recent past.[5,6,24,27,28] It has been already demonstrated that this strong layered arrangement is essential

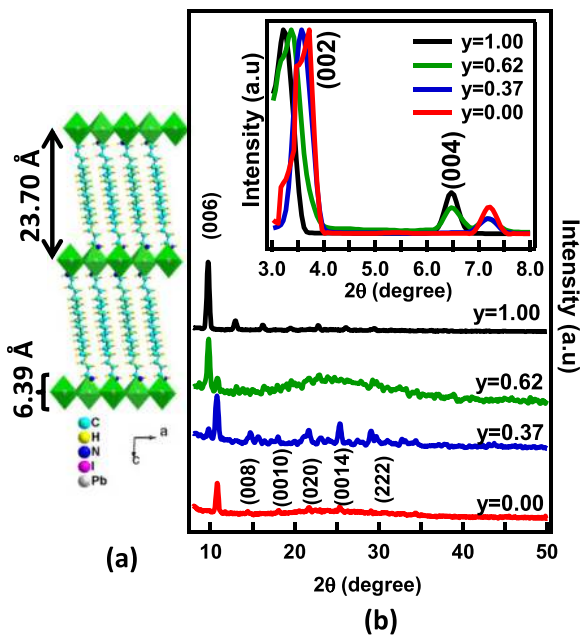

FIG. 1. (a) Schematic crystal structure packing representation[8,20] of IO hybrid, $(C_{12}H_{25}NH_3)_2PbI_4$ (C12PI). (b) X-ray diffraction pattern of C12PbI$_{4(1-y)}$Br$_{4y}$ ($y = 0$ to 1) thin films. Inset shows the shift in the characteristic peak (002).

for observing strong-room temperature excitons and the replacement of halides from I to Br and to Cl in the PbX_4 network does not alter the crystal packing and layering arrangement. Our thin films were carefully fabricated to obtain a high degree of directed X-ray reflections from the planes oriented stacked parallel to the c-axis. Therefore, their dominant *(002l)* reflections do not give further in-plane structural information.[29]

UV-Visible optical absorption and PL spectra of $C12PbI_{4(1-y)}Br_{4y}$ (y = 0–1) films measured at room-temperature are given in Figs. 2(a) and 2(b), respectively. These films exhibit narrow (~20–30 nm line width) and intense absorption bands between ~360 and 490 nm (Fig. 2(a)) and these peaks show a systematic shift towards higher energy with increasing Br content. Similar systematic shifts in the narrow exciton PL are observed (Fig. 2(b)). Compared to y = 0 (C12PI) and y = 1 (C12PB) compositions, the PL of mixed compositions at 0.37 and 0.62 show low intensity PL (18% and 42%, compared to y = 0).

Both parent PbI_2 and $PbBr_2$ are direct bandgap semiconductors with absorption edge near 2.5 eV and 4.0 eV, respectively.[30] The optical band gap (E_g) for the $C12PbI_{4(1-y)}Br_{4y}$ films has been estimated using the Tauc plots of the optical absorption spectra. From E_g and the peak position of the exciton absorption band (E_{abs}) the exciton binding energy ($E_{B.E}$) of mixed hybrid can be estimated, as $E_{B.E} \sim (E_g - E_{abs})$. According to this estimate, an increase in the binding energy of free excitons ranging from 220 to 310 meV has been obtained with this increase in *y* value. These excitonic binding energies are almost 10 times larger than that in PbI_2 (~30 meV). Such enhancement in the exciton binding energy is a consequence of a "dielectric confinement effect" and enables the excitons to appear even at room-temperature.[31,32]

The Stokes shift, the difference between the absorption and PL peak maxima ($\Delta E = E_{abs}$-E_{PL}), of $C12PbI_{4(1-y)}Br_{4y}$ films is minimum for y = 0 and 1 (50 meV, 90 meV), and reaches a maximum value for the mixed hybrid at y = 0.62 (up to 420 meV) (Fig. 2(e)) with the maximum line broadening of PL spectra (FWHM ~ 163 meV).

To examine the nature and physical/chemical morphology of $C12PbI_{4(1-y)}Br_{4y}$ mixed hybrid crystal surfaces, PL confocal microscopic imaging and room-temperature PL intensity spatial mapping has been performed. Results for one of the mixed hybrid crystal at y = 0.62 are shown in Figure 3. PL spectral scans have been performed over an area of 100 μm × 100 μm with 3 μm step sizes (Fig. 3(b)). To visualize any possible spectral variation at the crystal domains and at the edges, the PL spectra from line scans at particular X and Y directions are extracted from the PL spectral scans and presented in Figs. 3(c) and 3(d), respectively. As seen, the uniform single-line and unperturbed exciton PL

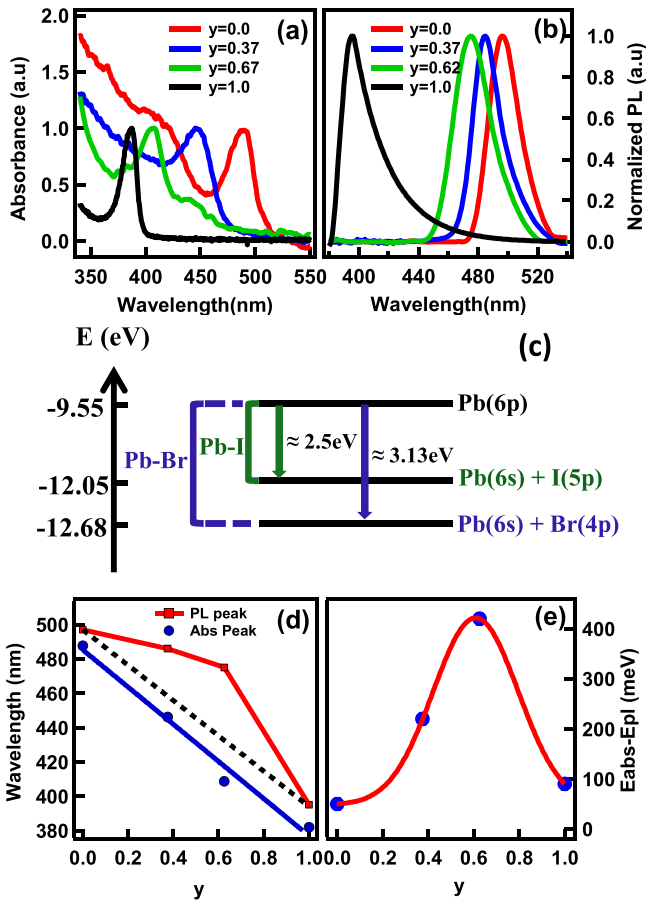

FIG. 2. (a) Optical absorption and (b) photoluminescence (PL) spectra of $C12PbI_{4(1-y)}Br_{4y}$ (y = 0–1) films measured at room temperature. (c) Schematic sketch of energy levels associated with the orbitals of Pb-I and Pb-Br bonds in $C12PbI_{4(1-y)}Br_{4y}$ system. Variation of (d) PL and absorption maxima with *y* composition and (e) Stokes shift, with the composition *y* of $C12PbI_{4(1-y)}Br_{4y}$. Solid lines are guide to the eye and dashed line is linear interpolation from y = 0 to y = 1, to represent imaginary composition *y′*.

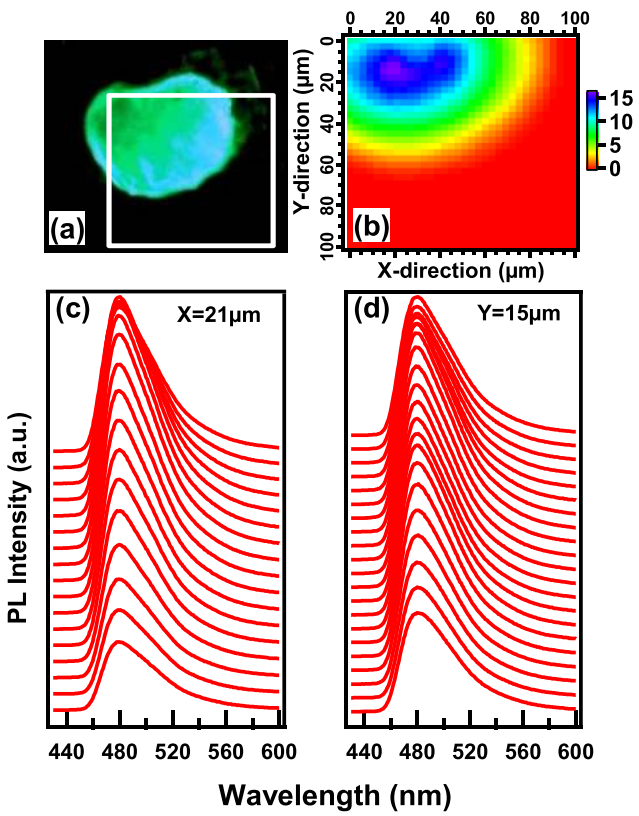

FIG. 3. (a) PL confocal microscopic image of $C12PbI_{4(1-y)}Br_{4y}$ (y = 0.62) crystal excited with 404 nm laser light, using LP > 410 nm filter. (b) Spatial PL intensity map (λ_{em} = 478 nm). (c) and (d) The spectral distribution along "X" and "Y" directions of the crystal respectively.

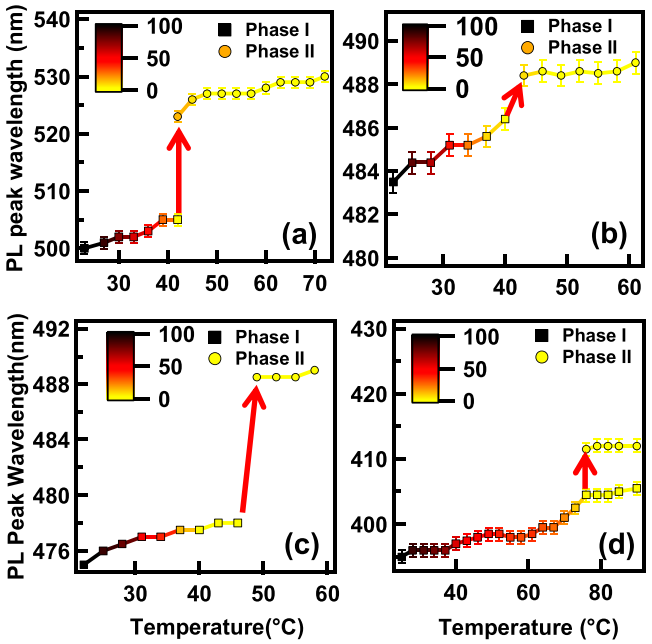

FIG. 4. Temperature dependence of PL maxima for $C12PbI_{4(1-y)}Br_{4y}$ thin films of (a) y = 0.0, (b) y = 0.37, (c) y = 0.62, and (d) y = 1.0. (The color scale shows the relative PL intensity in arbitrary units).

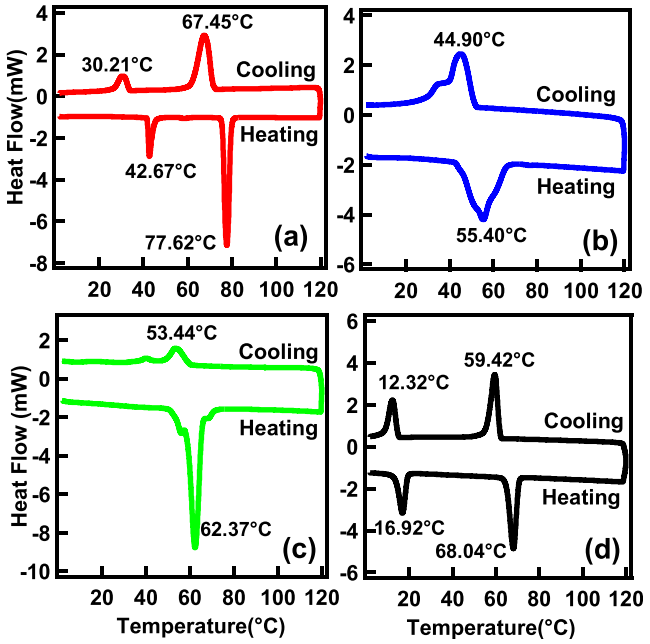

FIG. 5. DSC curves for powder samples of $C12PbI_{4(1-y)}Br_{4y}$ at (a) y = 0.0, (b) y = 0.37, (c) y = 0.62 and (d) y = 1.0. The cooling and heating scans are between 0 °C and 120 °C (5 °Cmin^{-1}).

($\lambda_{max} = 478$ nm) at room-temperature with no impurity or defect-related emission phase confirms the presence of a single phase of the mixed hybrid crystal at y = 0.62.

Since the long-alkyl chain containing IO hybrids are expected to show structural phase changes,[25,26] to study the effect of temperature and the related optical excitons in these mixed hybrids, temperature-dependent PL measurements were carried out between 22 °C and 90 °C in 3 °C temperature steps. As observed previously in the case of PbI_2 based hybrids,[25] these mixed hybrids also show a new red-shift of exciton PL peak at relatively high-temperatures. The PL maxima extracted over the full temperature range are plotted in Fig. 4 for the hybrids of various "y" compositions. Considerable red shift (up to 20 nm) between the low temperature (phase I) and high-temperature (phase II) excitons PL peaks are observed with a reversible critical cross-over at the phase transition temperature. Both these phases preserve excitonic features with narrow bandwidths below 30 nm in all the hybrids (y = 0 to 1). The critical phase transition occurs at a higher temperature as the Br content increases.

To study the corresponding thermal induced structural phases, Differential Scanning Calorimetry (DSC) traces for both cooling and heating runs for all mixed hybrids are recorded (Fig. 5) and relevant values are tabulated in Table I. All the compounds were found to show structural phase changes at a specific temperature with complete structural phase reversibility also observed. Both heating and cooling scans show respective endo- and exothermic transitions for all mixed compositions. In general for IO hybrids two significant endothermic (and exothermic) transitions are observed, with a minor one preceding each major one. Again both transition temperatures progressively shift to higher temperature as the *y*-composition value increases. Such phase transitions have been reported for higher-order alkyl ammonium chain based Pb(II) iodide hybrids, where the minor phase transition is referred to as "pre-melting" (T_1) and the major one is a "quasi-melting" (T_2) transition.[6,25,26,33] During the 1st phase transition (T_1), the structure transforms from orthorhombic to monoclinic crystal packing, whereas after the quasi-melting transition (T_2), a complete disordering and conformation of alkyl-ammonium chains is expected. Both these transitions are observed as exotherms upon cooling, with sign of thermal hysteresis as they occur at a lower temperature than their corresponding endotherms.[6] The tuning of T_1 and T_2 is discussed further below.

IV. DISCUSSION

The obtained results for the XRD patterns of thin films (Fig. 1) essentially show the layered perovskite structure, in

TABLE I. Differential scanning calorimetry (DSC) results for $C12PbI_{4(1-y)}Br_{4y}$(y = 0–1) hybrids showing phase transition temperatures (T_0, T_1, and T_2) and corresponding change in the enthalpies (ΔH_0, ΔH_1, and ΔH_2).

y-values	T_0 (°C)	ΔH_0 (J/g)	T_1 (°C)	ΔH_1 (J/g)	T_2 (°C)	ΔH_2 (J/g)
0.0						
Heating	–	–	42.67	8.94	77.62	37.78
Cooling			30.21	8.49	67.45	38.08
0.37						
Heating	–	–	55.40	54.53	–	–
Cooling			44.90	52.20		
0.62						
Heating	–	–	62.37	77.89	–	–
Cooling			53.44	16.80		
1.0						
Heating	16.92	15.38	68.04	27.57	–	–
Cooling	12.32	16.06	59.42	28.87		

which the 2D metal halide low-dimensional network and organic moieties (with ammonium termination) are alternately stacked along the *c*-axis. As clearly observed, the interlayer separation has been found to increase systematically as the Br content increases from $y = 0.0$ to 1.0. This can be predicted as due to the replacement of larger iodine atoms (atomic radius 140 pm) with relatively smaller bromine atoms (atomic radius 115 pm). As a result, the in-plane bending angles of Pb-X-Pb (X = I, Br) decrease[27,28] and at the same time the alkyl-ammonium chains conformation also changes from tilted geometry to a more upright position.[33] In these *c*-oriented hybrids, the selective replacement of I atoms with other halide atoms is of special interest since the metal halide layer arrangement is directly responsible for the structural as well as exciton energy level tuning.[25,26] For example, in PbX_4^{2-} systems, the replacement of halide (X^-) species from I^- to Br^- to Cl^-, tunes the excitons from 520 nm (for I^-) to 400 nm (for Br^-) to 280 nm (for Cl^-).[8,19–22] Therefore, selective replacement of I atoms with Br atoms causes substantial changes in the structural packing which further causes changes in optical band gap. Such studies will be discussed in the following sections.

Due to the influence of dielectric and quantum confinement effects, these layered perovskite exhibit sharp exciton peaks in the absorption and photoluminescence (PL) spectra at room-temperature.[34] It is generally accepted that the lowest fundamental optical transitions in $(RNH_3)_2PbX_4$ is similar to that of parent inorganic PbX_2.[35–37] In PbX_2, the top of the valence bands is composed of Pb(6*s*) orbitals hybridized with X(n, *p*) [where n = 5 for I and n = 4 for Br] orbital and the bottom of the conduction band is essentially of Pb(6*p*) character. The Br(4p) orbital energy is lower than that of the I(5p) orbital (Fig. 2(c)), hence the optical bandgap of Pb-Br hybrid systems are supposed to be larger than in Pb-I hybrids. In our recent works,[25,26,38] the optical bandgap values are directly correlated to the exciton transitions. Thus, it can be inferred that both excitonic absorption and PL shifts toward higher photon energy are due to active participation of substituting Br atoms in the band structure.

As observed in the absorption and PL measurements (Fig. 2(b)), the exciton emission maxima shifts non-linearly towards higher energy compared to the absorption maxima with increasing Br content. In the mixed crystal systems, the variation in the constituent atoms causes statistical fluctuations due to molecular level inhomogeneities. These fluctuations produce lattice strains, which are reflected in the Stokes shift and FWHM variations.[39–43] Few reports are available on binary mixed crystals of $A_{(1-y)}B_y$ type (including $PbI_{2(1-y)}Br_{2y}$ mixed crystals), which include studies of the effect of a linear variation of composition on the exciton energy, line-widths and changes in the exciton-phonon strengths.[40,42–45] In such systems, free-excitons and Self-Trapped Excitons (STE) can co-exist, and systematic studies of the dynamic variation of exciton relaxation due to changing exciton-phonon strengths have been presented. As mentioned earlier, the present IO mixed hybrids closely represents the parent binary alloy of $PbI_{2(1-y)}Br_{2y}$ and the discussion can also be conveniently extended to the mixed IO hybrid variation from C12PI (y = 0) to that of C12PB (y = 1). The exciton self-trapping in such mixed crystals can be visualized by taking account of both the exciton-phonon coupling strengths (the ratio between lattice relaxation energy to the exciton bandwidth) and potential alloy fluctuations (given by the ratio between trap depths (between I and Br sites) to the exciton line-widths). The difference in the band energies (Δ) of PbI_4^{2-} and $PbBr_4^{2-}$ can be considered as a short-range potential barrier. As the band energy of Pb-I networks is lower than that of Pb-Br, there is a potential barrier of height Δ around each Pb-Br site. Therefore, it is not energetically advantageous to distort the lattice at Pb-Br sites and an exciton self-trapping occurs at the available Pb-I network sites only, when the exciton-phonon coupling strength is large enough.[45] In such mixed circumstances, one would expect the net exciton absorption to arise from the extended non-localized excitons at all possible sites, while the Stokes-shifted broad emission is solely from the excitons of the lowest energy sites (Fig. 6(a)). This is why the PL and absorption then differ in the mixed alloys.

The diffusion and the probability distribution of excitons found in the relatively higher energy states corresponding to bromine rich sites compared to those in the lower energy states of pure iodine based sites, control our observations since such migration directly represents the difference in the absorption and PL energies. Fig. 6(b) represents a schematic *ab* plane view of a mixed inorganic network (Pb-I-Pb-Br) showing the suggested distribution of Br and I atoms at the bridging halide sites (anion sites) for a general mixed concentration. The excitons formed at the high energy Pb-Br sites are expected to diffuse towards the low energy Pb-I sites (as shown by arrows). However, the flux of diffusion depends on the presence of iodine rich and/or deficient units present on the mixed inorganic network. The absorption into the extended exciton states follows Vegard's Law with an energy which simply linearly interpolates between that in the two pure materials.[46,47] This implies that the extended exciton states are spatially large enough to average over local statistical fluctuations in the Br/I composition. On the other hand, the fact that the PL does not follow this trend means that it must arise from more localized exciton states which see more of the fluctuating in-plane potential from the Br/I composition (or its effect on the organic side-groups). Although the PL has indeed a broader linewidth from the mixed alloys, it is not spectrally centered about the linear interpolation between the PL lines of the pure materials. Hence local transport and migration of the excitons must occur followed by energy relaxation within the in-plane disorder potential. From Fig. 2(d), we see that the $y = 0.37$ PL emission appears to come from excitons in a local environment of $y = 0.22$. The in-plane Bohr radius of the exciton in these systems is estimated to be $a_B = 1.3$ nm,[48] which contains on average 8.6 Pb atoms and 47.3 anions. Assuming random filling of the individual anion sites with Br with probability $f = 0.37$, the probability that only a fraction $y' \approx 0.2$ of the $n = 47$ sites (i.e., $ny' \sim 10$ sites) are Br within the exciton is $p = \binom{n}{ny'} f^n (1-f)^{n(1-y')}$ which is less than 1% and only 1.6% have a fractional Br site within the exciton of 0.2 or less. This suggests that excitons must be able to migrate from their starting locations in either direction by

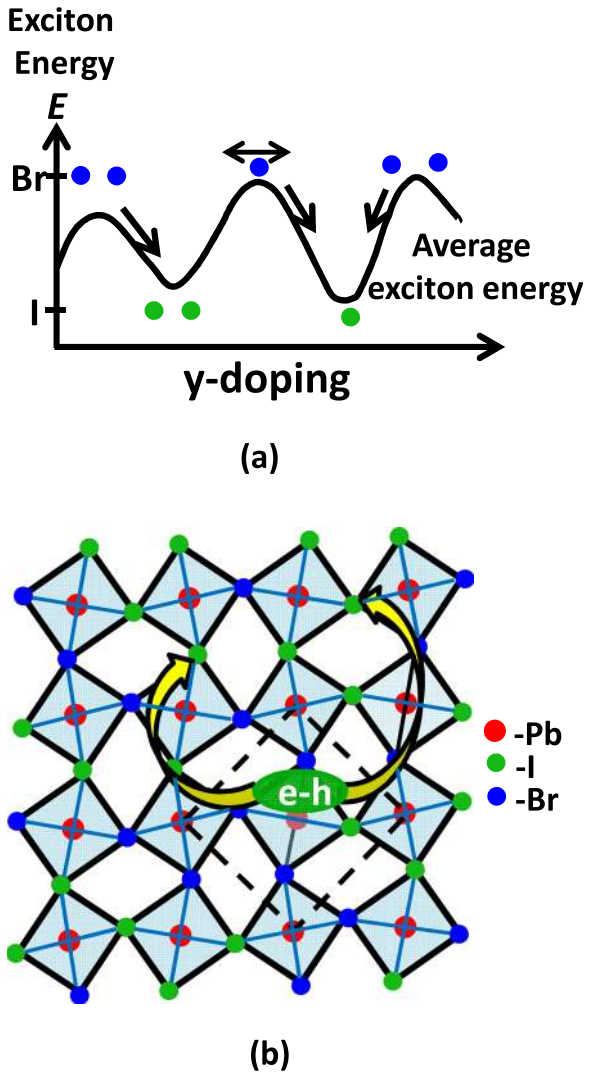

FIG. 6. (a) Schematic of exciton energy levels and the non-linear diffusion of excitons in mixed IO hybrids. (b) Schematic of Pb-I-Pb-Br network (top view) showing the diffusion of excitons from relatively high energy Pb-Br sites to lower energy Pb-I sites.

$l_d = a_B(0.016)^{-0.5} = 8a_B \sim 100$ Å, on average. Similarly for $y = 0.62$, the apparent Br site occupation from the PL is $y' \approx 0.35$. The estimated migration distance is then about 750 Å at this higher Br fraction (from an equivalent calculation). These are substantial exciton distances and are the first evidence for such transport in IO systems. The mechanism of exciton migration may be exciton diffusion through the corrugated energy landscape or it may be through emission/reabsorption events at different sites (a type of in-plane Forster transfer though virtual photons). These estimates however depend on the assumption of random alloy site filling. If there are correlations in the Br replacement, either in the different types of sites in which one is more important for the energy tuning, then different diffusion estimates will result. However for the current data without detailed site correlation information it is then not possible to extract more accurate exciton diffusion distances.

Apart from the structural engineering of Pb-X network and consequent excitonic emissions, these IO hybrids also give rise exciton flips due to structural phase transition within an IO hybrid. It has been recently demonstrated that the alkyl-chain based IO hybrids ($(C_nH_{2n+1}NH_3)_2PbI_4$,(for $n = 12,16,18$)) show temperature dependent structural phase-changes within accessible temperatures.[25,26] In the particular case of C12PI, a phase transition takes place at ~60 °C. The reason for such phase transformations can be understood by considering the arrangement of PbI_6 and organic moiety in C12PI (Fig. 7). The side-linked PbI_6 octahedra are extended as 2D planar sheets over (001) planes while, between PbI_6 octahedra, two organic moieties are coupled via N-H···I weak hydrogen bonds through the NH_3 ligands present at the terminal of the organic cation.[6,49] At room-temperature, the crystal packing of C12PI phase I is of stable orthorhombic phase (of space group *Pbca*)[8] while after 60 °C, the structure transforms into an phase II which is unstable phase of monoclinic with space group of $P2_1/a$.[6] At this phase change, the conformed alkylammonium chains within the PbI network changes from *trans* to *gauche* (or *vice versa*) arrangement. At the same time, Pb-I network organizes from relaxed network to a more crumpled network with in-plane Pb-I-Pb angles changes from 150.19° (phase I) to 157.42° (phase II).[6,25] In our recent communications,[25,26] it was predicted that the increased crumpling of inorganic sheets during the phase flips produce a blue shift in the bandgap, thus the exciton energies are systematically blue shifted.

However, in the case of mixed hybrids, the picture is a little different as the inorganic sheets contain both I and Br, hence the NH_3 ligands will form weak hydrogen bonds with

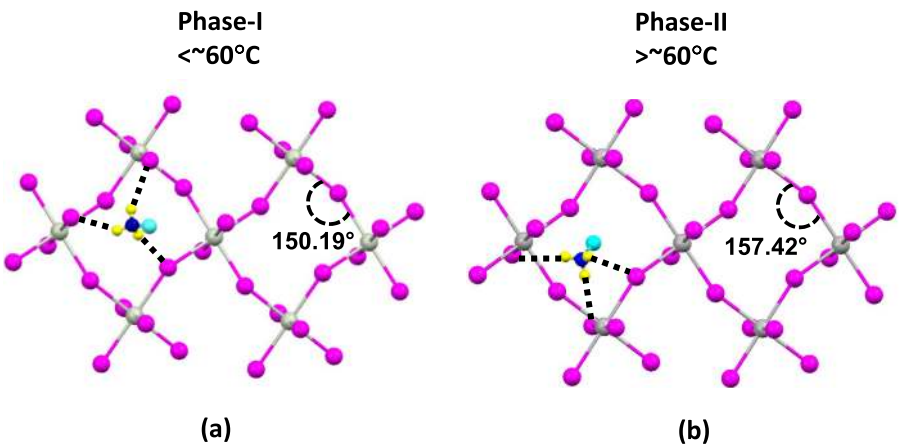

FIG. 7. Schematic representation of C12PI ($(C_{12}H_{25}NH_3)_2PbI_4$) IO hybrid crystal packing,[6,8] showing the in-plane Pb-I-Pb bond angles in (a) phase I (150.19°) and (b) phase II (157.42°).

both I and Br simultaneously. In order to explore such temperature dependent responses of excitonic features in such long alkyl-chain based mixed IO hybrids, thermal studies (exciton switching and DSC) of $C12PbI_{4(1-y)}Br_{4y}$ ($y = 0$–1) mixed hybrids have been obtained and the results from both the studies are discussed below.

As shown in Fig. 4, considerable exciton switching (up to 20 nm) at a particular transition temperature in all $C12PbI_{4(1-y)}Br_{4y}$ ($y = 0$–1) mixed hybrids. Both these low and high temperature excitons preserve their emission features with narrow bandwidths below 30 nm. Similar to C12PI ($y = 0$), in these mixed IO hybrids also the exciton switching can be understood as the result of reversible crumpling of the mixed inorganic Pb-X-Pb-X (X: I or Br) sheet networks. Further, the exciton switching temperature is found to be monotonically increasing with the increase in Br content.

According to the DSC data (Fig. 5), these alkylammonium chain based IO hybrids undergo multiple phase transitions out of which two phase transitions are dominant within the temperature range of 0 ° to 120 °C as:

$$y = 0.00 \;:\; C12PI(I) \underset{30.21^{\circ}C}{\overset{42.67^{\circ}C}{\rightleftharpoons}} C12PI(II) \underset{67.45^{\circ}C}{\overset{77.62^{\circ}C}{\rightleftharpoons}} C12PI(III)$$

$$y = 1.00 \;:\; C12PB(0) \underset{12.32^{\circ}C}{\overset{16.92^{\circ}C}{\rightleftharpoons}} C12PB(I) \underset{59.42^{\circ}C}{\overset{68.04^{\circ}C}{\rightleftharpoons}} C12PB(II) \underset{>120^{\circ}C}{\overset{>120^{\circ}C}{\rightleftharpoons}} C12PB(III).$$

Considering the phase transition temperature T_1 (pre-melting: phase I to phase II) in the case of mixed hybrid states at $y = 0.37$ (55.40 °C) and 0.62 (62.37 °C) (Fig. 5), a systematic shift has been observed towards the higher temperature end.

The first (or pre-melting: phase I to phase II) phase transitions exhibits considerable thermal hysteresis, showing a prominent structural transformation and the second (or quasi-melting: phase II to phase III) is accompanied by dilation of the lattice parameters with possibility of crystallinity loss.[6,25,26] For displacive phase transition (pre-melting) the enthalpy (Table I) is less than that for the second phase transition, where the alkylammonium chains can show dynamical disorder along their longitudinal axis, leading ultimately to a "quasi-melting" of the hydrocarbon component. The phase transition temperature (T_1) for all the hybrids shows a linear increase with the increase in the composition value y. At $y = 1.0$ (C12PB) a new phase transition peak appears at 16.92 °C (T_0), which is thought to be a new low-temperature phase transition (phase 0 to phase I).[50] The phase transitions obtained from DSC are compared with the phase transition obtained from PL exciton switching measurements (Fig. 4) are compared in Figure 8. The phase transitions obtained from PL measurements, recorded between the range of between 22 °C and 90 °C, are in close agreement with the pre-melting phase transition temperature (T_1) variation obtained from DSC studies.

Though the crystal packing in all y composition retains the layered structure arrangement during the phase transformation at T_1, the systematic increase in the thermal energy required for phase flips suggests that the inorganic layer network arrangement plays a more crucial role compared to the alkyl chain conformation within the layers. The large shift in the phase transition temperature (T_1) from $y = 0.0$ to 1.0 can be attributed to the fact that the bond energy for Pb-Br bond (201 $kJ.mol^{-1}$) is higher than that of Pb-I bond (142 $kJ.mol^{-1}$) system. In intermediate systems, more energy is required to produce effective changes in the bond angles of Pb-Br-Pb compared to Pb-I-Pb in the mixed Pb-X-Pb-X (X: I or Br) sheets. For $y = 0.62$, most of the terminal halide positions are possibly occupied by Br atom therefore the structure is relatively more stable than $y = 0.37$, wherein the terminal halide positions are randomly occupied by either I or Br atoms.[51] Hence, the phase transition in $y = 0.37$ takes place at relatively lower temperature (55.4 °C) than $y = 0.62$ (62.4 °C). In general, these studies demonstrate the significance of the structural phase transitions both optically and thermally. This study also provides comprehensive information regarding suitable working ranges of temperature for these mixed hybrid materials when utilized in optoelectronic devices. However, the relation between structural/thermal

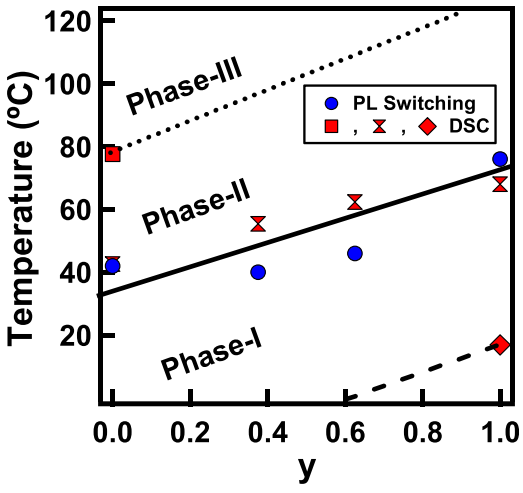

FIG. 8. Variation of phase transition temperatures obtained from PL peak switching studies and DSC (heating run) and with different y-value of $C12PbI_{4(1-y)}Br_{4y}$. The lines are guide to the eye, the dotted line (….) indicates T_2, the solid line indicates T_1 and the dashed line (- - - - -) indicates T_0 transition temperatures.

results and the exciton behavior cannot be fully explained unless the crystal structures of these mixed hybrids are better known and understood.

V. CONCLUSIONS

In conclusion, the structural, optical and thermal properties of novel inorganic–organic phase-change crystalline hybrids $C12PbI_{4(1-y)}Br_{4y}$ ($y = 0$ to 1) have been systematically studied and reported. Structural characterization using techniques such as X-ray make it possible to correlate structural features with specific materials properties such as optical and thermal functionality. These naturally self-assembled systems adopt layered structures, where inorganic and organic networks are alternately stacked along the *c*-axis. The successive Br substitution in the Pb-I inorganic network results in variation in inorganic network crumpling and interlayer spacing due to the variation in the in-plane bending angles from Pb-Br-Pb network to Pb-I-Pb. These hybrids possesses strong and narrow room-temperature excitonic features that can be tuned from green to blue upon increase of the Br content, in the Pb-I network, making them a potential candidate for use in optoelectronic devices. The large Stokes shift observed between exciton absorption and PL emission energies in the intermediate compositions is attributed to the local transport and migration of excitons from higher energy Pb-Br sites to the lower energy Pb-I sites. By considering the applicability of Vegard's law in the mixed crystal system substantial exciton migration distances for Br-dominant hybrids have been estimated by assuming random alloy site filling. Furthermore, these systems show reversible exciton switching behaviour, arising from the reversible crumpling of the Pb-X (I or Br) network at easily accessible structural phase transition temperatures. The DSC experiments further confirm the structural phase-changes and evidence complete phase reversibility in these mixed IO hybrids. For practical application of mixed IO hybrids in optoelectronic device applications such structural, optical, thermal and further correlative studies are of special importance. Not only do these studies present the limits of working temperature ranges of devices for optimal optoelectronic activity but also provide information regarding the choice of mixed IO hybrid material with desired properties.

ACKNOWLEDGMENTS

This work is part of High-Impact Research scheme of IIT Delhi, Nano Research Facility (MCIT, Govt. of India), DST-SERB (Govt. of India) funding, *UK-India Education and Research Initiative* (UKIERI) programme, and part funded by EPSRC Grant Nos. EP/G060649/1 and ERC LINASS 320503.

[1]D. B. Mitzi, S. Wang, C. A. Field, C. S. Chess, and A. M. Guloy, Science **267**, 1473 (1995).
[2]C. R. Kagan, D. B. Mitzi, and C. D. Dimitrakopoulos, Science **286**, 945 (1999).
[3]K. S. Aleksandrov and V. V. Beznosikov, Phys. Solid State **39**, 695 (1997).
[4]G. C. Papavassiliou, Prog. Solid State Chem. **25**, 125 (1997).
[5]D. B. Mitzi, Prog. Inorg. Chem. **48**, 1 (1999).
[6]D. G. Billing and A. Lemmerer, New J. Chem. **32**, 1736 (2008).
[7]E. Hanamura, N. Nagaosa, M. Kumagai, and T. Takagahara, Mater. Sci. Eng. B **1**, 255 (1988).
[8]K. Pradeesh, G. Sharachandar Yadav, M. Singh, and G. Vijaya Prakash, Mater. Chem. Phys. **124**, 44 (2010).
[9]H. Arend, W. Huber, F. H. Mischgofsky, and G. K. Richter-Van Leeuwen, J. Cryst. Growth **43**, 213 (1978).
[10]M. Shinada and S. Sugano, J. Phys. Soc. Jpn. **21**, 1936 (1966).
[11]Y. Masumoto and M. Matsuura, Phys. Rev. B **32**, 4275 (1985).
[12]M. Era, S. Morimoto, T. Tsutsui, and S. Saito, Appl. Phys. Lett. **65**, 676 (1994)
[13]K. Pradeesh, J. J. Baumberg, and G. Vijaya Prakash, Opt. Express **17**, 22171 (2009).
[14]K. Shibuya, M. Koshimizu, Y. Takeoka, and K. Asai, Nucl. Instrum. Methods Phys. Res. B **194**, 207 (2002).
[15]B. Radisavljevic, A. Radenovic, J. Brivio, V. Giacometti, and A. Kis, Nature Nanotech. **6**, 147 (2011).
[16]Q. H. Wang, K. Kalantar-Zadeh, A. Kis, J. N. Coleman, and M. S. Strano, Nature Nanotech. **7**, 699 (2012).
[17]Z. Xu and D. B. Mitzi, Inorg. Chem. **42**, 6589 (2003).
[18]Z. Xu, D. B. Mitzi, C. D. Dimitrakopoulos, and K. R. Maxcy, Inorg. Chem. **42**, 2031 (2003).
[19]J. Calabrese, N. L. Jones, R. L. Harlow, N. Herron, D. L. Thorn, and Y. Wang, J. Am. Chem. Soc. **113**, 2328 (1991).
[20]N. Kitazawa, K. Enomoto, M. Aono, and Y. Watanabe, J. Mater. Sci. **39**, 749 (2004).
[21]N. Kitazawa, M. Aono, and Y. Watanabe, Thin Solid Films **518**, 3199 (2010).
[22]D. B. Mitzi, K. Chondroudis, and C. R. Kagan, IBM J. Res. Dev. **45**, 29 (2001).
[23]G. Vijaya Prakash, K. Pradeesh, R. Ratnani, K. Saraswat, M. E. Light, and J. J. Baumberg, J. Phys. D **42**, 185405 (2009).
[24]S. Zhang, G. Lanty, J. Lauret, E. Deleporte, P. Audebert, and L. Galmiche, Acta Mater. **57**, 3301 (2009).
[25]K. Pradeesh, J. J. Baumberg, and G. Vijaya Prakash, Appl. Phys. Lett. **95**, 173305 (2009).
[26]K. Pradeesh, J. J. Baumberg, and G. Vijaya Prakash, J. Appl. Phys. **111**, 013511 (2012).
[27]D. G. Billing and A. Lemmerer, Cryst. Eng. Commun. **9**, 236 (2007).
[28]D. G. Billing and A. Lemmerer, Cryst. Eng. Commun. **11**, 1549 (2009).
[29]N. V. Venkataraman, S. Bhagyalakshmi, S. Vasudevan, and R. Seshadri, Phys. Chem. Chem. Phys. **4**, 4533 (2002).
[30]A. F. Malysheva and V. G. Plekhanov, Opt. Spectrosc. **34**, 302 (1973).
[31]A. M. Guloy, Z. Tang, P. B. Miranda, and V. I. Srdanov, Adv. Mater. **13**, 833 (2001).
[32]M. Shimizu, J. Fujisawa, and J. Ishi-Hayase, Phys. Rev. B **71**, 205306 (2005).
[33]S. Barman, N. V. Venkataraman, S. Vasudevan, and R. Seshadri, J. Phys. Chem. B **107**, 1875 (2003).
[34]Y. Kawabata, M. Yoshizawa Fujita, Y. Takeoka, and M. Rikukawa, Synth. Met. **159**, 776 (2009).
[35]T. Ishihara, J. Takahashi, and T. Goto, Phys. Rev. B **42**, 11099 (1990).
[36]I. B. Koutselas, L. Ducasse, and G. C. Papavassiliou, J. Phys. Condens. Matter **8**, 1217 (1996).
[37]M. Hirasawa, T. Ishihara, and T. Goto, J. Phys. Soc. Jpn. **63**, 3870 (1994).
[38]K. Pradeesh, K. Nageswara Rao, and G. Vijaya Prakash, J. Appl. Phys.**113**, 083523 (2013).
[39]J. I. Pankove, *Optical Processes in Semiconductors* (Dover Publication, New York, 1971), p. 114, Chap. 6.
[40]A. Naumov, H. Stanzl, K. Wolf, S. Lankes, and W. Gebhardt, J. Appl. Phys. **74**, 6178 (1993).
[41]R. W. Martin, P. G. Middleton, K. P. O'Donnell, and W. Van der Stricht, Appl. Phys. Lett. **74**, 263 (1999).
[42]Y. Shinozuka and Y. Toyazawa, J. Phys. Soc. Jpn. **46**, 505 (1979).
[43]N.Kitazawa, J. Phys. Soc. Jpn. **36**, 2272 (1997).
[44]J. Takeda, T. Tayu, S. Saito, and S. Kurita, J. Phys. Soc. Jpn. **60**, 3874 (1991).
[45]Y. Shinozuka, J. Phys. Soc. Jpn. **59**, 1322 (1990).
[46]L. Vegard, Z. Phys. **5**, 17 (1921).
[47]R. Butté *et al.*, J. Phys. D **40**, 6328 (2007).
[48]N. A. Gippius, E. A. Muljarov, S. G. Tikhodeev, T. Ishihara, and L. V. Keldysh, in *MRS Proceedings*, Vol. 328, p. 775 (1993).
[49]D. B. Mitzi, Chem. Mater. **13**, 3283 (2001).
[50]P. Vanek, M. Havrankova, and J. Hybler, Solid State Commun. **82**, 509 (1992).
[51]H. Abid, A. Samet, T. Dammak, A. Mlayah, E. K. Hlil, and Y. Abid, J. Lumin. **131**, 1753 (2011).